

## MEASUREMENT OF WEB SURFACE PROFILES USING FRINGE PROJECTION

By

Hongbing Lu, Vinay Bhumannavar, Junfeng Liang, and Yao Ren  
Oklahoma State University  
USA

### ABSTRACT

In this paper a full-field measurement technique, namely fringe projection technique was implemented to determine the three-dimensional surface profile for situations where webs are opaque or translucent. In this method, a grating is projected to the surface of a web. The projected grating will be distorted due to the non-flat surface. The image of the distorted gratings will be shifted on a reference grating on a computer to form Moiré fringes. The phase of the fringes is determined and converted to the surface profile of the web. Calibration was conducted, and validation was made on surfaces with known geometry. Surface profiles of Polyvinyl Fluoride (PVF), nonwoven and polyethylene webs, as well as non-flat side walls of a wound roll determined as examples illustrating the technique. The accuracy of the method is discussed. The method has potential for industrial scale applications due to its ease in setup and speed in three-dimensional reconstruction.

### NOMENCLATURE

$d$	distance between the camera and the projector, mm
$f$	frequency of projected fringes
$f_0$	frequency of generated fringes
$I(x,y)$	grayscale distribution
$I_o(x,y)$	grayscale distribution on object image
$I_r(x,y)$	grayscale distribution on reference image
$k$	calibration constants, mm/rad
$l$	distance between the camera and the reference plane, mm
$p$	pitch of the fringes
$z(x,y)$	surface height, mm
$\theta$	angle between projection and observation axes, rad
$\Phi$	phase value, rad
$\Delta\Phi$	phase difference, rad

## INTRODUCTION

Webs wound into rolls can develop defects during winding, and eventually translate into roll defects. These defects may be broadly classified as web defects and roll defects, such as baggy lanes and wound roll edge offsets. Baggy lanes may appear in the form of camber, wrinkles, etc., and are the cause for many problems encountered in converting and winding processes [1]. Web defects arise mostly due to improper winding conditions such as poor winding tension control, roller misalignment, etc. In addition to these factors, improper nip, poor core strength, low torque on driving roller, etc. may result in roll defects. Measurements of these defects as well as quality control often need to measure the surface profiles. For example, wrinkling is avoided by closely monitoring the winding tension using load cells, while roll defects such as roll edge offsets are measured by go/no-go gages [2]. More precise measurements of web planarity and roll quality require installation of expensive machinery, which is not only cumbersome, time consuming and difficult to operate. Due to these difficulties, on many occasions rolls have to be shipped to a different location in order to have their quality characterized.

Several optical measurement techniques are capable of the full-field, non-contact, three-dimensional surface profiling. Examples of these techniques include the Moiré method [3], the holographic method [4] and the fringe projection technique [5]. Among these methods, fringe projection technique is inexpensive and flexible in dealing with different object sizes, different surface finish and complex shapes. The sensitivity and range can be adjusted by changing the parameters in the system. Moreover, the fringe projection technique does not require highly precise alignment of the optical elements [3]. In fringes projection technique, a sinusoidal fringe pattern is projected onto the surface of the object. The projected fringes will be distorted due to the height change of the surface. The phase changes modulated in the distortion of the fringes can be calculated and transformed into the height values of the object. In combination with the digital projection techniques, by using the digital display device such as Digital-Light-Processing (DLP) projector or Liquid-Crystal-Display (LCD) projector as the fringe projector, different fringe patterns can be easily generated and accurately controlled by the computer.

In the present work, we use the digital fringe projection technique to provide an accurate, low cost and simple solution to measure the surface profiles for a web. A non-contact, full-field measurement method employing the digital fringe projection technique to detect, measure, and reconstruct three-dimensional surface profiles of webs and rolls is presented. As an illustration, wrinkles on PVF and translucent polyethylene and nonwoven webs and wound roll offsets are measured. In this study, the method developed by M. Heredia and E.A. Patterson for phase extraction and unwrapping will be used [3]. The method has the potential for industrial applications in that it provides an accurate and efficient way for the measurements.

## PRINCIPLE

Figure 1 shows a schematic digital fringe projection setup. Fringe patterns are generated by a computer, projected through a digital projector onto the object whose surface profile will be measured. A digital camera is used to record an image for the distorted fringes on the object. The depth information can be extracted by phase analysis of the fringe patterns.

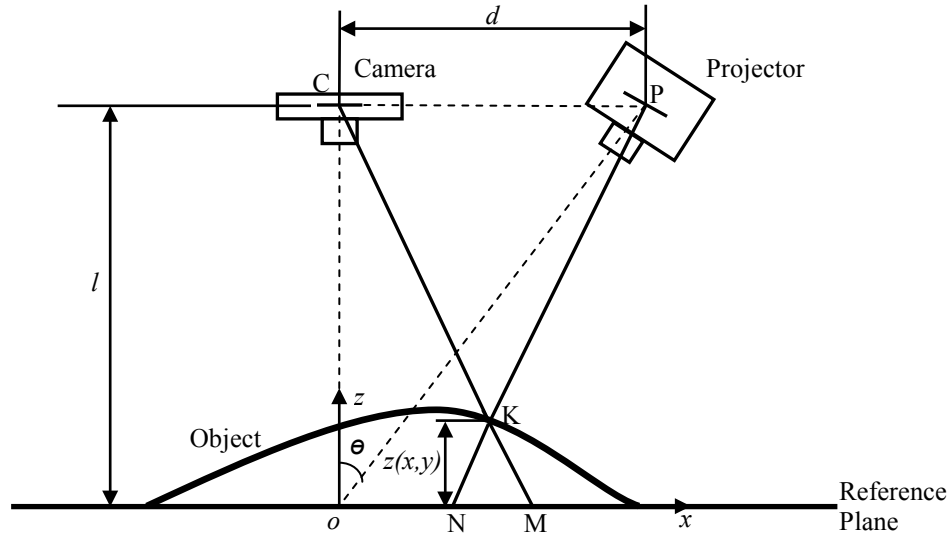


Figure 1 – Schematic diagram of a fringe projection setup

### **Phase–Depth Relationship**

As shown in Figure 1, a reference plane is located at the intersection of optical axes of the projector and the camera, and is perpendicular to the camera axes. A Cartesian coordinate system is then established with the origin at the intersection  $o$ ,  $x$  axis towards right,  $y$  axis normal to the figure plane and  $z$  axis towards the camera. The depth of the reference plane is identically zero in the  $z$  direction. All the measurements are relative to this plane. Fringes with the grayscale distribution expressed as in equation {1} are projected onto the reference plane. Two images are captured: one is the reference image with projected fringes pattern on the reference plane, the other one is the object image with the fringes pattern projected on the object.

$$I(x, y) = \frac{1}{2}(1 + \cos(2\pi f_0 x)) \quad \{1\}$$

where  $f_0$  is the carrier frequency of the fringe. If width of the pitch is  $p$ ,  $f_0$  is given as:

$$f_0 = \frac{1}{p} \quad \{2\}$$

The grayscale distributions of the two images acquired can be expressed as

$$I_r(x, y) = A_r(x, y) + B_r(x, y) \cos[2\pi f_0 x + \Phi_r(x, y)]$$

$$I_o(x, y) = A_o(x, y) + B_o(x, y) \cos[2\pi f_0 x + \Phi_o(x, y)] \quad \{3\}$$

where  $A_i$  and  $B_i$  represent the variations of the background illumination and fringe modulation,  $\Phi_r$  and  $\Phi_o$  are the phase values of any pixel on reference image and object image, respectively. If the camera optical axis has an angle  $\theta$  with respect to optical axis of the projector, then

$$f = f_o \cos \theta \quad \{4\}$$

Consider an arbitrary point K on the object surface, it has coordinates  $(x_K, y_K)$  with depth  $z(x_K, y_K)$ . From the camera imaging plane, K will be viewed as point M,

$$(x_K, y_K) = (x_M, y_M) \quad \{5\}$$

From the observation from the projector, phase of point K in the object image is identical to the phase of point N in the reference image, combined with equation {5}, the phase value is equal to that of point M, expressed as

$$\Phi_r(x_N, y_N) = \Phi_o(x_K, y_K) = \Phi_o(x_M, y_M) \quad \{6\}$$

Therefore, phase difference between M and N can be computed simply by subtracting phase of the same point between the reference image and the object image, expressed as

$$\Delta\Phi_{MN} = \Phi_r(x_M, y_M) - \Phi_r(x_N, y_N) = \Phi_r(x_M, y_M) - \Phi_o(x_M, y_M) = \Delta\Phi_{ro} \quad \{7\}$$

Phase difference between M and N is encoded with the distance information and can be converted into depth by geometry relationship. Based on the fact that  $\Delta MKN$  is similar to the  $\Delta CPK$ , if  $l \gg z(x_K, y_K)$ , we have

$$z(x_K, y_K) = \frac{MN}{d} (l - z(x_K, y_K)) \cong \frac{MN}{d} l \quad \{8\}$$

On the reference plane, the length of MN is related with the phase difference between M and N as

$$MN = \frac{1}{2\pi f} \Delta\Phi_{MN} \quad \{9\}$$

Therefore, substituting equations {7}, {8} into {9}, the final expression for the depth of any point K is

$$z(x_K, y_K) = \frac{l}{2\pi f d} \Delta\Phi_{ro} = k \Delta\Phi_{ro} \quad \{10\}$$

where

$$k = \frac{l}{2\pi f d} \quad \{11\}$$

From equation {10}, we know that  $k$  is a constant determined by the assignment of the optical components and fringe pitch. If the same fringes are projected, after the positions of all the components are fixed,  $k$  remains a constant. This constant will be determined during calibration.

### **Phase Measurement**

Based on the relationship between phase difference and depth, if we know the phase value for every point on the reference image and object image, the depth of every point on object can be measured, and hence we have the profile for the object. The key process is the measurement of phase value. There are different algorithms developed in the past for phase extraction. Among these algorithms, spatial carrier phase-stepping methods [6] allow the measurement of the phase from a single object image with a very low computational expense. Therefore, the phase measurement software, JOSHUA, used in this study takes the following self-calibrating five-step phase estimator for temporal phase shifting [6], and adapts it for spatial phase stepping

$$\Phi = \arctan\left(\frac{2(I_2 - I_4)}{2I_3 - I_5 - I_1}\right) \quad \{12\}$$

where  $I_i (i=1,2,3,4,5)$  represent five images shifted from a single image on a computer. The acquired image is shifted in the direction perpendicular to the fringes by different ratios of fringe pitch, expressed as:

$$\begin{aligned} I_1 &= I(i, j - \text{int}(p/2)) \\ I_2 &= I(i, j - \text{int}(p/4)) \\ I_3 &= I(i, j) \\ I_4 &= I(i, j + \text{int}(p/4)) \\ I_5 &= I(i, j + \text{int}(p/2)) \end{aligned} \quad \{13\}$$

The phase extraction algorithm is then applied respectively to reference image and object image to obtain the phase value of every point on each image.

### **Phase Unwrapping**

The phase value calculated through equation {12} is wrapped within  $[-\pi, \pi]$ , which will produce a  $2\pi$  discontinuity in depth values. Phase unwrapping algorithm is used to detect the jumps in phase value and add multiples of  $2\pi$  to make a continuous phase map. For 2D phase unwrapping methods, a main problem is that small error in phase value will propagate and accumulate through the image to produce a failure. The software, JOSHUA, uses a quality bins algorithm, which processes the phase unwrapping from the area with best data quality to that of lower data quality. This technique restricts the error in limited region.

## EXPERIMENTAL PROCEDURE

### Apparatus

Figure 2 shows an image of the experimental setup used in this study. The experimental setup consists of a projector used to project fringes onto the object of interest, a camera used to acquire images of reference and distorted fringes, a laser level to maintain alignment, and a computer for data processing. In order to provide for easy reproducibility, the setup was developed using a commercially available projector, Infocus 120 DLP projector. A Nikon D70 DSLR camera with 18–70 mm lens with an external trigger was used to acquire images of the fringes. A Black and Decker 10 in. line laser generator was used to align the projection surface perpendicular to the camera axis. The fringes were produced on a computer using MATLAB to have the sinusoidal grayscale distribution. An aluminum frame was built to support an MFB wood board, which formed the plane for reference fringes.

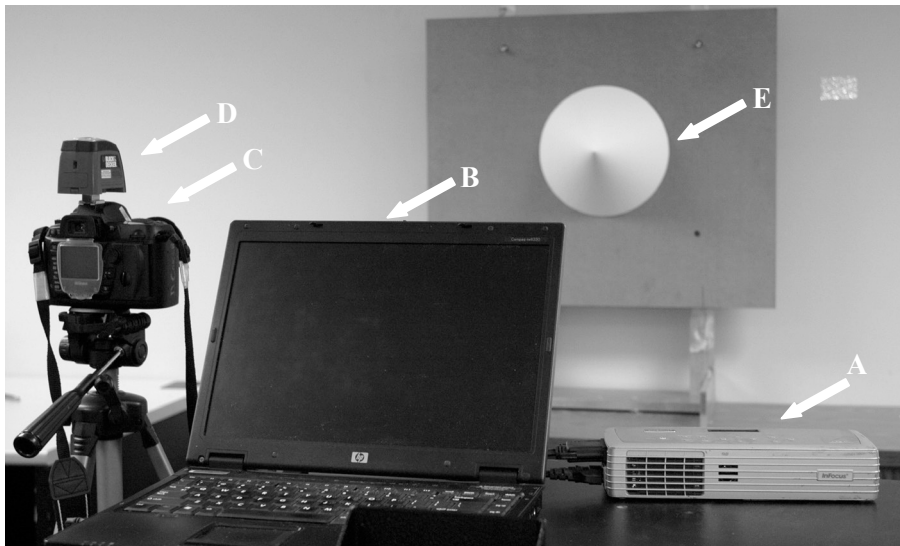


Figure 2 – Experimental setup: A– Digital Light Processing projector; B– Processing computer; C– CCD camera; D– Alignment laser; E– Calibration cone.

### Procedure

**Calibration:** The calibration constant, in equation {11}, for conversion from the phase to depth is determined by calibration using optical parameters and fringe pattern. To determine this constant, the system is used to measure some objects with known geometry. In this study, a cone was chosen as the calibration shape for its simple geometry, which is easy to manufacture and to describe mathematically with only two parameters (i.e. the height and the radius). It was found on repeated trials that in order for the measurement method to be effective, the size of cone used for calibration should not be grossly different from that of the feature being profiled [3]. A series of models with different dimensions and shapes are made to do the calibration and validation, as shown in Figure 3. Table 1 contains the dimensions of the models, the diameters and side lengths were measured by a digital micrometer and the height was measured by height gauge.

Further, the surface of the cone needs to have optimum reflectivity. A highly reflective surface would render high noise, whereas a very low reflective surface would not give bright object image. Therefore, white flat paints are used to color the surface of these models. A reference image and an image with fringes projected onto the cones were acquired, following which, the height and base diameter values of the cone were entered into the software. This allows the software to calculate the calibration constant. Figure 4 shows the images used in calibration process.

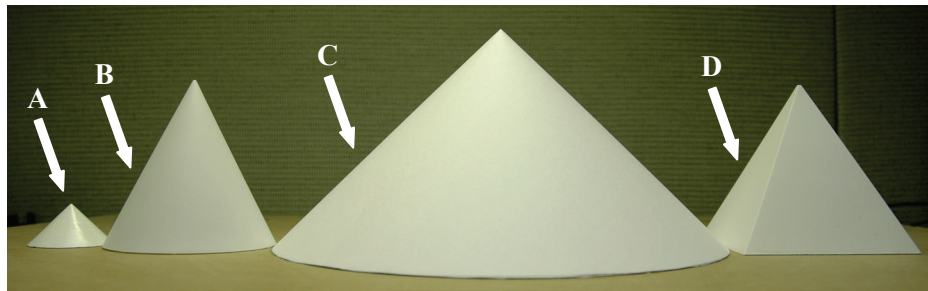


Figure 3 – Models used in this study: A– Cone 1; B– Cone 2; C– Cone 3; D– Pyramid

Model	Radius (mm)	Height (mm)
Cone 1	24.87	25.54
Cone 2	52.53	104.75
Cone 3	139.38	135.51
Pyramid	104.85	104.85

Table 1 – Dimension of models used in the experiment

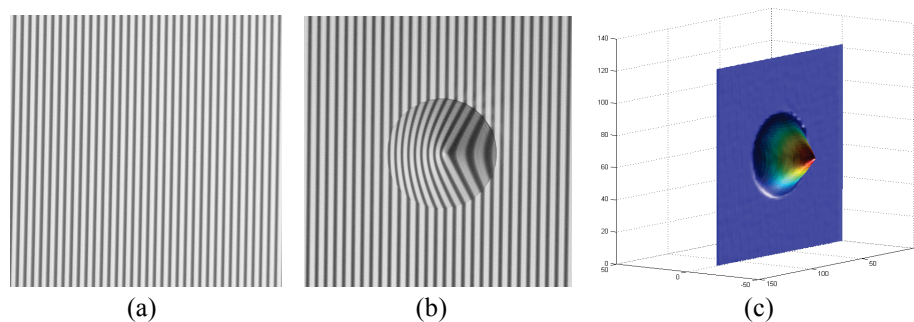


Figure 4 – Calibration using Cone 1: A– Reference image; B– Cone 1 with fringes projected; C– Three–dimensional reconstruction of Cone 1

**Validation:** In order to determine the accuracy of the fringe projection technique and to validate the system and the calibration process, a validation process was conducted. In this process, every cone is used as a calibration object and the rest of models are measured to show the accuracy. Table 2 shows the results. When Cone 1 is used as the calibration object, the measured height of Cone 3 has an error of 7.05%. And conversely, if Cone 3 is used to in calibration, the height of Cone 1 has an error of 4.07%. This indicates that there would be a relatively larger error when the calibration object and the object being measured have a large difference in dimensions. When Cone 2 was used as

the calibration object, all the relative errors were under 5% and it showed a great accuracy of 99.5% and 99.36% for profiling surfaces of Cone 3 and Pyramid respectively.

Calibration Model	Measured Model	Measured Height (mm)	Relative Error
Cone 1	Cone 2	99.7897	-4.74%
	Cone 3	125.9535	-7.05%
	Pyramid	100.3525	-4.29%
Cone 2	Cone 1	24.7272	3.18%
	Cone 3	134.8338	-0.50%
	Pyramid	105.5086	0.63%
Cone 3	Cone 1	24.4998	-4.07%
	Cone 2	106.4061	1.48%
	Pyramid	107.7463	2.76%

Table 2 – Validation Results

**Measurement:** In order to ensure that good images are acquired for the Moiré interferometry, an optimal level of fringe width is required. It is important that the projected fringes be equally spaced on a computer, and also on the surface of the reference plane. The processing algorithm involves Fourier phase transformations, the fringes should follow a sinusoidal pattern with gradual change in grayscale. As the measurement of the object of interest is relative to the reference image, it is important that the setup remains undisturbed after calibration until the measurement process is complete. For the measurement of wrinkles, PVF, nonwoven and polyethylene web specimens were subjected to a uniaxial tensile stress on an Instron tensile tester at an extension rate of 0.423 mm/s. The PVF and the polyethylene web specimens have a length of 723.9 mm, width of 152.4 mm and were subjected to a strain of 1.75%, while the nonwoven web was 381.0 mm in length, 152.4 mm in width, and was subjected to a strain of 3.3%. In calibration, Cone 1 attached to a plastic board was placed in front the plane on which a web specimen would be placed, while the plastic board served as the reference plane. The fringe width was 7 pixels per fringe. A second image was recorded by projecting the fringes on to the wrinkles and Moiré interferometry was performed using the JOSHUA software. Due to the translucence of the polyethylene and nonwoven web, fringe patterns would become less clear and leads to poor quality in the reconstructed geometry. After several attempts, we found that a combination using the maximum brightness of the projector and a black background behind the web sample solved the problem. For the measurement of roll defects, a PVF roll was wound with specified amount of core offset to illustrate the capability to measure offset defects. In this instance, calibration was conducted using Cone 3 supported on a wooden board attached on an aluminum frame. A fringe width of 8 pixels per fringe was used. A second image was acquired by projecting fringes on to the rolls placed right next to the reference plane. Three-dimensional geometry reconstruction was then performed by using the software. The results of analysis in each of the instances are given as follows.

## RESULTS

### Measurement of Wrinkles

The technique successfully reconstructs the wrinkles on PVF web, as shown in Figure 5. A selected region of 644×1484 pixels, corresponding to an area of 150.0×345.8 mm, from the object image is chosen for the purpose of reconstruction, as illustrated in figure 5 (a). The number and shape of wrinkles obtained by reconstruction of surface profile is in

good agreement with that observed during the experiment. Figure 6 shows the depth distribution along the width, about 15 pixels from the top of the image. Because the reference plane was located in front of the web sample, the depth values in the plot was subtracted by that positive offset distance to compensate for position of reference plane. The height can give us a clear view of the shape of wrinkles. The curve clearly presents 4 wrinkles, of which the first three has similar amplitudes while the last one has a larger amplitude. This irregularity may be attributed to some misalignment of the top and bottom clamps.

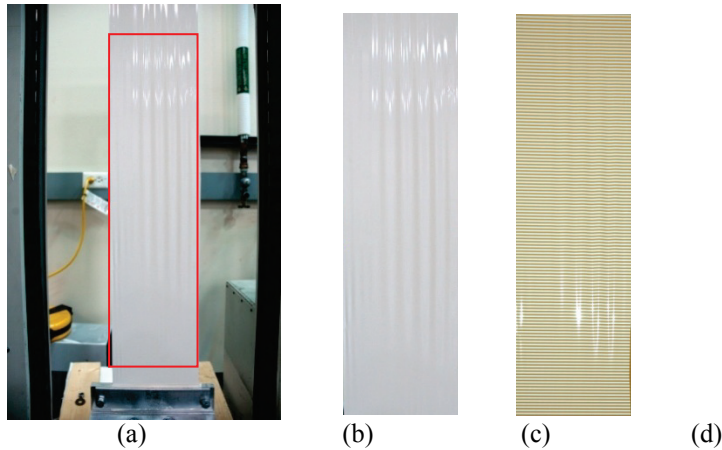


Figure 5 – Reconstruction of the PVF web wrinkles. (a): PVF web on the Instron machine; (b) PVF web wrinkles; (c) PVF web wrinkles with projected fringes; (d): reconstruction of the PVF web wrinkles.

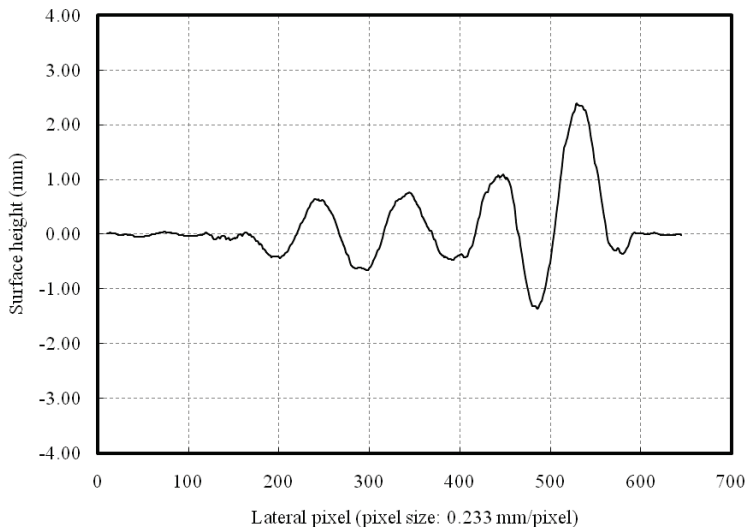


Figure 6 – Surface height along the cross line

Figure 7 shows the reconstruction of the nonwoven web subjected to the tensile test. The reconstruction was based on a selected region of 364×1500 pixels, corresponding to

an area of  $84.8 \times 349.5$  mm, shown in Figure 7 (a). As shown in Figure 7 (b), the size of wrinkles generated was relatively small and localized at certain areas. The reconstructed image in Figure 7 (d) confirmed the same phenomena. The coarseness of the web surface contributes to a less smooth reconstruction, while the translucence results in partial loss of information in the images captured.

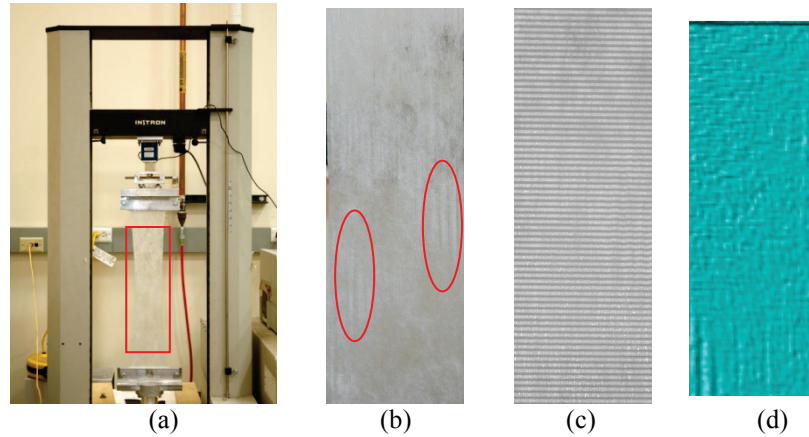


Figure 7 – Reconstruction of the nonwoven web wrinkles. (a): web sample on the Instron machine; (b) nonwoven web wrinkles; (c) web wrinkles with projected fringes; (d): reconstruction of the nonwoven web wrinkles.

Figure 8 shows the reconstruction of a translucent polyethylene web during the uniaxial tensile test. As shown in Figure 8 (b), five wrinkles were formed in the center region of the web sample. The reconstruction by the software indicated the same surface profile as shown in Figure 8 (d).

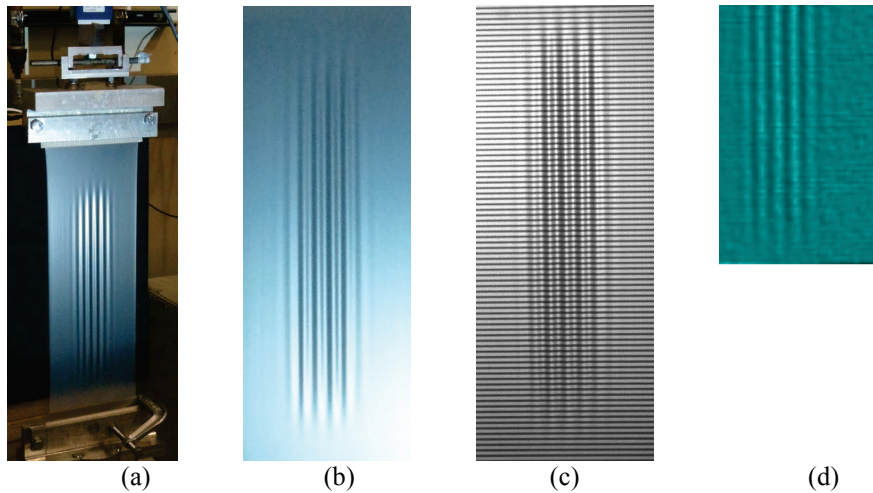


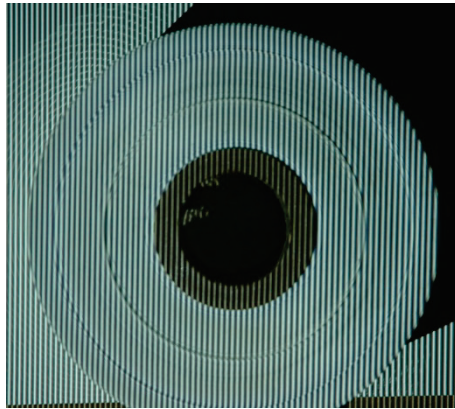
Figure 8 – Reconstruction of the polyethylene web wrinkles. (a): web sample on the Instron; (b) web wrinkles; (c) web wrinkles with projected fringes; (d): reconstruction of the web wrinkles.

The method therefore is fairly sensitive and has potential to not only measure wrinkles, but also aid in investigation of various causes for wrinkling. This technique can also be used as an effective troubleshooting tool in controlling parameters that affect web quality during winding.

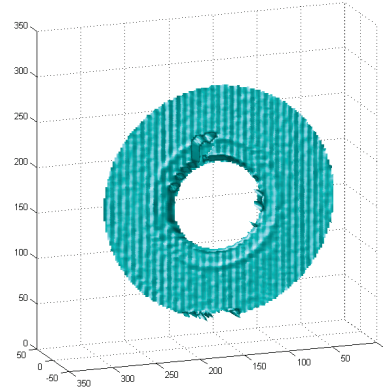
#### **Measurement of the Roll Side Surface**

The measurement of defects in rolls requires consideration of certain parameters such as fringe width, intensity variation of fringes. To illustrate the importance of the effect of these parameters, a comparative study was made selecting different fringe densities. A fringe width of 12 pixels per fringe was used for projection. The reconstruction of the edge surface profile observed was poor, with certain amount of details either missing or corrupted as shown in Figure 9 (b). It is also noteworthy that steep changes are difficult to detect, owing to loss of fringe data in the shadow produced as a result of steepness of the feature. The existence of shadow makes it hard for phase unwrapping to continue, as a result, the reconstruction of that part was not made.

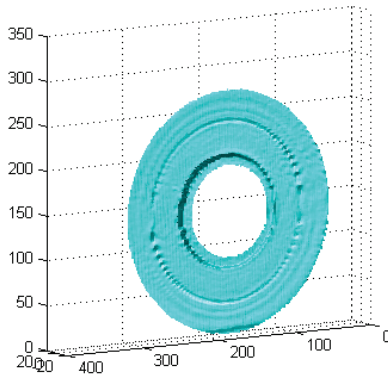
Subsequent trials performed involved optimization of these parameters to obtain a smoother and more accurate contour of the edge surface. For fringe densities of 6 pixels per fringe or less, it is difficult to produce sinusoidal fringes owing to the small number of pixels in each fringe. A fringe width of 8 pixels per fringe was formed to be optimal. MATLAB was used to generate fringes with step change in intensities, and the focus of the projector was adjusted a little out of focus to produce sinusoidal fringes. Significant improvements in the results were observed. The reconstructed profile is shown in Figure 9 (c). Certain rolls were observed to have periodic offsets from the edge. The technique therefore possesses potential in creating large number of opportunities to observe such defects in real time, and control the parameters which cause the defects.



(a)



(b)



(c)

Figure 9– Reconstruction of the side wall of a roll. (a) Image of fringes projected on a roll; (b) Poor reconstruction of side wall due to improper fringe parameters; (c) Reconstruction after optimization of parameters.

## CONCLUSION

A non-contact, full-field measurement system using the digital fringe projection technique was used to detect, measure, and reconstruct three-dimensional surface profiles of webs and rolls. The system, constructed by using a commercially available projector, digital camera and computer, has the capability to determine three-dimensional surface profiles. Examples are given to reconstruct the wrinkles formed on webs and to characterize wound roll offsets. The method has the potential for a wide range of web handling applications as it provides an accurate, low cost and efficient way for three-dimensional profiling.

## ACKNOWLEDGMENTS

The authors would like to thank Professor Ken Belanus at Department of Mechanical Engineering Technology, Oklahoma State University (OSU) for his help in preparation of large cones. We are grateful to Mr. John Gage at the Design and Manufacturing Labs, OSU for his help in development of cones and frame. We acknowledge the support of the Web Handling Research Center at OSU.

## REFERENCE

1. Roisum, D. R., "Baggy Webs: Making, Measurement and Mitigation Thereof," 2001.
2. Good, J. K. and Roisum, D. R., "Winding: Machines, Mechanics and Measurements," TAPPI Press, 2008.
3. Takasaki, H., "Moiré Topography," Applied Optics, Vol. 9, 1970, pp. 1467–1472.
4. Thalmann, R. and Dandliker, R., "Holographic Contouring Using Electronic Phase Measurement," Optical Engineering, Vol. 24, 1985, pp. 930–935.
5. Ortiz, M. H. and Patterson, E. A., "Location and Shape Measurement Using a Portable Fringe Projection System," Society for Experimental Mechanics, 45(3), 2005, pp.197–204.
6. Chan, P. H. and Bryanston–Cross, P. J., "Spatial Phase–Stepping Method of Fringe Pattern Analysis," Optics and Lasers in Engineering, Vol. 23, 1995, 343–354.

*Measurement of Web Surface Profiles  
Using Fringe Projection*

**H. Lu, V. Bhumannavar, J.  
Liang, & Y. Ren,** Oklahoma  
State University, USA

**Name & Affiliation**

**Question**

No Questions until Discussion